



Contents lists available at ScienceDirect

Physica A

journal homepage: www.elsevier.com/locate/physa

Influence of the interaction range on the thermostatics of a classical many-body system

Leonardo J.L. Cirto^{a,*}, Vladimir R.V. Assis^b, Constantino Tsallis^{a,c}

^a Centro Brasileiro de Pesquisas Físicas and National Institute of Science and Technology for Complex Systems, Rua Xavier Sigaud 150, 22290-180 Rio de Janeiro-RJ, Brazil

^b Departamento de Física, Universidade Estadual de Feira de Santana, 44031-460 Feira de Santana-BA, Brazil

^c Santa Fe Institute, 1399 Hyde Park Road, Santa Fe, NM 87501, USA

HIGHLIGHTS

- Detailed molecular dynamics study for the HMF and the α -XY models is presented.
- Both short- and long-range regimes are analyzed and different behaviors are shown.
- For the short-range regime the results agree with standard statistical mechanics.
- In the long-range case the results points to nonextensive statistical mechanics.

ARTICLE INFO

Article history:

Received 30 August 2013

Available online xxxx

Keywords:

Metastable state

Long-range interaction

Ergodicity breaking

Nonextensive statistical mechanics

ABSTRACT

We numerically study a one-dimensional system of N classical localized planar rotators coupled through interactions which decay with distance as $1/r^\alpha$ ($\alpha \geq 0$). The approach is a first principle one (*i.e.*, based on Newton's law), and yields the probability distribution of momenta. For α large enough and $N \gg 1$ we observe, for longstanding states, the Maxwellian distribution, landmark of Boltzmann–Gibbs thermostatics. But, for α small or comparable to unity, we observe instead robust fat-tailed distributions that are quite well fitted with q -Gaussians. These distributions extremize, under appropriate simple constraints, the nonadditive entropy S_q upon which nonextensive statistical mechanics is based. The whole scenario appears to be consistent with nonergodicity and with the thesis of the q -generalized Central Limit Theorem.

© 2013 Elsevier B.V. All rights reserved.

1. Introduction

More than one century ago, in his historical book *Elementary Principles in Statistical Mechanics* [1], J. W. Gibbs remarked that systems involving interactions such as Newtonian gravitation are intractable within the theory proposed by Boltzmann and himself, due to the divergence of the canonical partition function. This is of course the reason why no standard temperature-dependent thermostatical quantities (*e.g.*, a specific heat at finite temperatures) can possibly be calculated for the free hydrogen atom, for example. Indeed, although the quantum approach of the hydrogen atom solves the divergence associated, for classical gravitation, with small distances, the divergence associated with large distances remains the same. More precisely, unless a box surrounds the atom, an infinite number of excited energy levels accumulate at the ionization value, which yields a divergent canonical partition function at any finite temperature. This and related questions are commented on in Ref. [2], for instance.

* Corresponding author. Tel.: +55 21 2141 7223; fax: +55 21 2141 7223.

E-mail addresses: cirto@cbpf.br (L.J.L. Cirto), vladimir@cbpf.br (V.R.V. Assis), tsallis@cbpf.br (C. Tsallis).

Here we report a numerical study of the α -XY model [3], a many-body Hamiltonian system with two-body interactions whose range is controlled by a parameter of the model. More precisely, we assume a potential which decays with distance as $1/r^\alpha$ ($\alpha \geq 0$). This model recovers, when $\alpha = 0$, the Mean Field Hamiltonian (HMF), a fully coupled many-particle system [4], and recovers, in the $\alpha \rightarrow \infty$ limit, the first-neighbor XY ferromagnet, a model which is well defined within the traditional thermostatical scenario of short-range interactions. Systems with long-range interactions have been attracting particular attention of the statistical-mechanical community in the last two decades. This renewed and increasing interest was launched by Antoni and Ruffo in 1995 [4] with their discussion of the HMF model, which in many aspects mimics traditional long-range systems while bypassing some of its difficulties.

The model focused on here was introduced some years later in Ref. [3]. It is a direct generalization of the HMF by including a power-law dependence on distance in order to control the range of the interactions.¹ We refer to short-range (long-range) interactions when the potential felt by one rotator of a d -dimensional system is integrable (nonintegrable), i.e., when $\alpha/d > 1$ ($0 \leq \alpha/d \leq 1$). A direct consequence of this fact is that the total energy is extensive when $\alpha/d > 1$, whereas it is superextensive if $0 \leq \alpha/d \leq 1$. As we shall numerically illustrate, for large values of α/d the system exhibits the standard behavior expected within Boltzmann–Gibbs (BG) statistical mechanics. However, we shall also exhibit that when long-range interactions become dominant, i.e., when $\alpha/d < 1$, the situation is much more complex. In 1988 a generalization of the BG statistical mechanics based on a different entropic functional [2,6,7] was proposed. Within this approach, the thermodynamical structure (free energy, temperature, etc.) can be extended [2,8–11]. Some of the numerical results presented in the next sections appear to be in close agreement with this theory.

2. The model

To transparently extract the deep consequences of Gibbs’ remark, in the present paper we focus on the influence of the range of the interactions within an illustrative isolated classical system, namely the α -XY model [3]. This model consists of a d -dimensional hypercubic lattice of N interacting planar rotators, whose Hamiltonian is given by

$$\mathcal{H} = \frac{1}{2} \sum_{i=1}^N p_i^2 + \frac{1}{2} \sum_{i=1}^N \sum_{\substack{j=1 \\ j \neq i}}^N \frac{1 - \cos(\theta_i - \theta_j)}{r_{ij}^\alpha} \quad (\alpha \geq 0), \tag{1}$$

with periodic boundary conditions. Each rotator is characterized by the angle $\theta_i \in [0, 2\pi)$ and its canonical conjugate momentum p_i . Without loss of generality we have considered unit moment of inertia, and unit first-neighbor coupling constant; r_{ij} measures the (dimensionless) distance between rotators i and j , defined as the minimal one given the periodic boundary conditions.

For $d = 1$, r_{ij} takes the values $1, 2, 3, \dots$; for $d = 2$, it takes the values $1, \sqrt{2}, 2, \dots$; for $d = 3$, it takes the values $1, \sqrt{2}, \sqrt{3}, 2, \dots$. Notice that, in contrast with Newtonian gravitation, the potential in Hamiltonian (1) does not diverge at short distances since the minimal distance, in any dimension, is always the unit. The kinetic term in (1), proportional to p_i^2 , is the traditional one, but the interaction term is long-range for $\alpha \leq d$, which makes the internal energy per particle to diverge in the thermodynamic limit. Following [12], this property can be seen by realizing that the energy *per particle* of the interaction term varies with N like [13,14]:

$$\tilde{N} \equiv \frac{1}{N} \sum_{i=1}^N \sum_{\substack{j=1 \\ j \neq i}}^N \frac{1}{r_{ij}^\alpha} = \sum_{j=2}^N \frac{1}{r_{1j}^\alpha}. \tag{2}$$

In the $\alpha \rightarrow \infty$ limit, $\tilde{N} = 2d$. If $\alpha/d < \infty$, the discussion of the above sum can be conveniently replaced by the discussion of the following integral [3]:

$$d \int_1^{N^{1/d}} dr \frac{r^{d-1}}{r^\alpha} = \frac{N^{1-\alpha/d} - 1}{1 - \alpha/d}, \tag{3}$$

which behaves, when $N \rightarrow \infty$, like $N^{1-\alpha/d}/(1-\alpha/d)$ if $0 \leq \alpha/d < 1$, like $\ln N$ if $\alpha/d = 1$, and like $1/(\alpha/d - 1)$ if $\alpha/d > 1$. In other words, the total internal energy is extensive (in the thermodynamical sense) for $\alpha/d > 1$, and nonextensive otherwise. In order to accommodate to a common practice, we can rewrite the Hamiltonian \mathcal{H} as follows [3]:

$$\bar{\mathcal{H}} = \frac{1}{2} \sum_{i=1}^N p_i^2 + \frac{1}{2\tilde{N}} \sum_{i=1}^N \sum_{\substack{j=1 \\ j \neq i}}^N \frac{1 - \cos(\theta_i - \theta_j)}{r_{ij}^\alpha} = K + V, \tag{4}$$

which can now be considered as “extensive” for all values of α/d , at the “price” that a microscopic two-body coupling constant becomes now, through N , artificially dependent on N . However, as shown in Ref. [3], this corresponds in fact

¹ We refer the reader to the work by Chavanis and Campa [5], where a quite complete list of references about the evolution of this subject can be found.

to a rescaling of time (hence of p_i).² More precisely, this rewriting takes into account the fact that, for all values of α/d , the thermodynamic energies (internal, Helmholtz, Gibbs) grow like NN , the entropy, volume, magnetization M , number of particles, etc., grow like N (i.e., remain extensive for both regions above and below $\alpha/d = 1$), and the temperature T , pressure, external magnetic field, chemical potential, etc., must be scaled with N in order to have finite equations of states [2]. The correctness of this (conjectural) scaling was numerically shown in Ref. [13] for the present specific $d = 1$ system, and has been profusely verified in the literature for several other systems, e.g., in ferrofluid [12], fluid [15], magnetic [16–18], diffusive [19], percolation [20,21] systems, among others (see Ref. [2] for an overview). Also, it was analytically proven [14] (see also [22]), for any d and $0 < \alpha < d$, that rewriting (4) associates to the α -XY model the same behavior as that, previously known, of the $\alpha = 0$ [4] case. This universality is clearly exhibited by plotting T/\tilde{N} and M versus $\langle \mathcal{H} \rangle / N\tilde{N}$ for different values of α and N as in Ref. [13], or, equivalently, T and M versus $\langle \tilde{\mathcal{H}} \rangle / N$ as in Refs. [14,23].

2.1. The cases $\alpha = 0$ and $\alpha \rightarrow \infty$

Eq. (4) unifies two models that have been frequently studied separately, namely the cases $\alpha = 0$ and $\alpha \rightarrow \infty$. The particular instance $\alpha = 0$ recovers the HMF model [4]. If we conveniently note the potential V as V_α , we straightforwardly verify that the HMF potential corresponds to

$$V_0 = \frac{1}{2N} \sum_{i=1}^N \sum_{j=1}^N [1 - \cos(\theta_i - \theta_j)]. \quad (5)$$

The restriction $i \neq j$ is not necessary anymore, and we have approximated $\tilde{N} = N - 1 \sim N$. The other particular case corresponds to first-neighbor interactions. Indeed, if we take the $\alpha \rightarrow \infty$ limit in Eq. (4) and considering periodic boundary conditions we obtain:

$$V_\infty = \frac{1}{2} \sum_{i=1}^N [1 - \cos(\theta_i - \theta_{i+1})]. \quad (6)$$

The partition function for the first-neighborhood potential (6) was calculated by Mattis [24] using the transfer matrix technique. The caloric curve (T vs. u) is therefore straightforwardly obtained. For our purpose here it is sufficient to recall that, for $u = 0.69$, $T \approx 0.7114$. This value was correctly recovered in our numerical simulations for α sufficiently large, as exhibited in Fig. 1 for $\alpha = 10.0$.

3. Short- and long-range regimes: Lyapunov exponents

At the fundamental state, all rotators are parallel, say $\theta_i = 0$, $\forall i$, which corresponds to the ferromagnetically fully ordered case. At high enough energies, the values of $\{\theta_i\}$ are randomly distributed, which corresponds to the paramagnetic phase. In between, for $\alpha < d$, a second order phase transition occurs at a critical temperature $T_c = 1/2$ corresponding to a critical energy $u_c = 3/4$ [4,14]; the order parameter is the vector magnetization $\mathbf{M} = 1/N \sum_{i=1}^N \mathbf{m}_i$, where $\mathbf{m}_i = (\cos \theta_i, \sin \theta_i)$.

In addition to the above, it has already been shown that, at the special value $\alpha/d = 1$, frontier between the long- and short-range regimes, the dynamical behavior sensibly changes. Indeed, for $N \rightarrow \infty$ and energies corresponding to the paramagnetic region, the largest Lyapunov exponent of the many-body system remains finite and positive for $\alpha/d > 1$, whereas it gradually vanishes for $0 \leq \alpha/d \leq 1$. It vanishes like $N^{-\kappa}$, where $\kappa(\alpha/d)$ decreases from a positive value (close to $1/3$) to zero when α/d increases from zero to 1, and remains zero for $\alpha/d \geq 1$. It is interesting to emphasize that κ does not independently depend on (α, d) , but only on the ratio α/d [3,25,26]. Consistently with the fact that, for all values of the energy per particle u in the paramagnetic region, the Lyapunov exponents vanish in the limit $N \rightarrow \infty$, κ does not depend on u .

4. Numerical procedure and results

Let us present now the microcanonical molecular-dynamical results that we have obtained for the $d = 1$ Hamiltonian (4) with fixed (N, u) , the total energy being Nu . To integrate the $2N$ equations of motion we used the Yoshida 4th-order symplectic algorithm [27,28] with an integration step chosen in such a way that the total energy is conserved within a relative fluctuation smaller than 10^{-5} . Some of our present results were also checked through the standard Runge–Kutta scheme. The class of the initial configurations that we run is the so-called water-bag: all rotators started with the same angle $\theta_i = 0$, $\forall i$, and each momentum p_i is drawn at random from a uniform distribution. We rescaled all the p_i 's in order to precisely achieve the total desired energy u as well as zero total angular momentum, resulting in a uniform distribution with width $2\sqrt{6u}$ and zero mean.

² If we take into account that the momentum p_i involves a derivative with respect to time t , $\dot{\theta}_i = \frac{\partial \mathcal{H}}{\partial p_i} = p_i$, we verify that $\mathcal{H} = \tilde{N}\tilde{\mathcal{H}}$ provided that t is replaced by $\tilde{t} = \sqrt{\tilde{N}}t$.

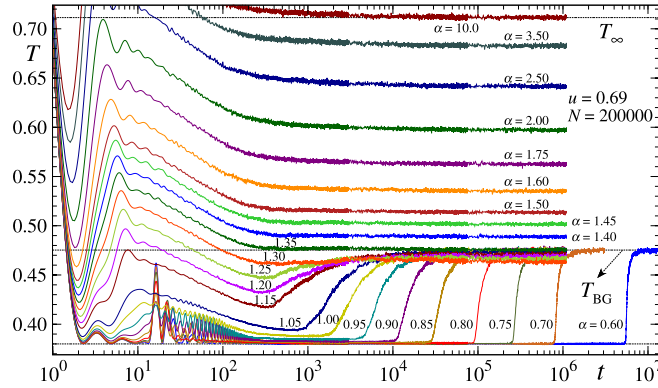


Fig. 1. Time dependence of the kinetic temperature $T(t) \equiv 2K(t)/N$ for a water bag typical single initial condition for $(u, N) = (0.69, 200\,000)$ and various values of α . The upper horizontal line, at $T_\infty = 0.7114 \dots$, corresponds to the BG thermal equilibrium temperature of the $\alpha \rightarrow \infty$ model at, $u = 0.69$ [24]. The middle (lower) horizontal line, at $T \simeq 0.475$ ($T = 0.380$), indicates the BG thermal equilibrium temperature (the QSS base temperature, corresponding to zero magnetization), at $u = 0.69$ and $0 \leq \alpha < 1$ [4,14]. In the range $1 \leq \alpha < \infty$, no analytical solution is available, as far as we know.

4.1. Temperature and momentum distribution

We present in Fig. 1 the instantaneous kinetic “temperature” $T(t) \equiv 2K(t)/N$, where $K(t)$ is the time-dependent total kinetic energy of Hamiltonian \mathcal{H} . As verified many times in the literature, a quasi-stationary state (QSS) exists for $0 \leq \alpha/d < 1$ and $u \simeq 0.69$, after which a crossover is observed to a state whose temperature coincides with that analytically obtained within Boltzmann–Gibbs (BG) statistical mechanics [4,23]. Sufficiently after the QSS period, whose lifetime appears to diverge with increasing N , the kinetic temperature of the system fluctuates around its BG value as time increases. The temporal mean value calculated within this stable region is noted $T_{\text{kin}} \equiv \langle T(t) \rangle = \langle 2K(t)/N \rangle$, and is represented by the full red points in Fig. 4.

It has been long thought that, after this crossover, the system consistently adopts a BG distribution in Gibbs Γ space, and therefore a Maxwellian distribution for $P(p_i)$. The facts that we now present reveal a much more complex situation, where robust q_n -Gaussians (or distributions numerically very close to them) emerge before the crossover (just before for most realizations of the initial conditions, but also quite a lot before for some of them) and remain so for huge times (as long as our longest runs); n stands for *numerical*. This unexpected phenomenon occurs for u both below and above $u_c = 3/4$, and for α both below and above $\alpha = 1$ (up to $\alpha \simeq 2$). Let us emphasize that these q_n -Gaussians only develop their full shape if sufficient time has been run in order that the apparently stationary state has been attained. This time is extremely long for $0 < u \ll 3/4$ because the system is then almost integrable (indeed, the Hamiltonian can be straightforwardly checked to become very close to that of N coupled harmonic oscillators, by using $\cos(\theta_i - \theta_j) \sim 1 - \frac{1}{2}(\theta_i - \theta_j)^2$), and is also extremely long for $u \gg 3/4$ because once again the system is almost integrable (indeed, the Hamiltonian can be straightforwardly checked to become now very close to N independent localized rotators). Let us detail now how the single-initial-condition one-momentum distributions $P(p)$ are calculated within large time regions where T is nearly constant: for each value of i , we register its p_i at very many (noted n) successive times separated by an interval τ , and then, following the recipe of the Central Limit Theorem (and of its q -generalization [29–34]), we calculate its arithmetic average \bar{p}_i (thus corresponding to the interval $t \in [t_{\text{min}}, t_{\text{max}}]$ with $t_{\text{max}} - t_{\text{min}} = n\tau$). We then plot the histogram for the N arithmetic averages, as illustrated in Fig. 2. Notice that the CLT recipe is nothing but a time average, which frequently corresponds in fact to real experiments.

4.2. q -Kurtosis

All the histograms that we have obtained for sufficiently large times t are well fitted with $e_{q_n}^{-\beta_{q_n} p^2/2}$, with (q_n, β_{q_n}) depending on (α, u, N, τ) as well as on $(t_{\text{min}}, t_{\text{max}})$ where $e_q^x \equiv [1 + (1 - q)x]^{1/(1-q)}$ ($q \in \mathcal{R}$; $e_1^x = e^x$) [2,35]. To check the quality of the fit we introduce (see Fig. 3) a conveniently q -generalized kurtosis (referred to as q -kurtosis), defined as follows (see Ref. [36] and references therein):

$$\kappa_q = \frac{\int_{-\infty}^{\infty} dp p^4 [P(p)]^{2q-1} / \int_{-\infty}^{\infty} dp [P(p)]^{2q-1}}{3 \left[\int_{-\infty}^{\infty} dp p^2 [P(p)]^q / \int_{-\infty}^{\infty} dp [P(p)]^q \right]^2}, \tag{7}$$

where we have used the escort distributions. Escort distributions were, as far as we know, introduced in 1995 by Beck and Schögl [37] and play a particular role in nonextensive statistical mechanics [2,38]. The mean values associated with these distributions have the remarkable advantage of being finite up to $q = 3$, which is precisely the value below which q -Gaussians are normalizable, i.e. $\int_{-\infty}^{\infty} dp P_0 e_q^{-\beta_{q_n} p^2/2} = 1$ ($q < 3$). The use of the standard kurtosis $\kappa_1 = \langle p^4 \rangle / 3 \langle p^2 \rangle^2$ when the probability distribution is a q -Gaussian has the considerable disadvantage that $\langle p^2 \rangle$ diverges for $q \geq 5/3$, and $\langle p^4 \rangle$ diverges for $q \geq 7/5$. Hence κ_1 becomes useless for $q \geq 7/5$, and it happens that some of the distributions that we observe

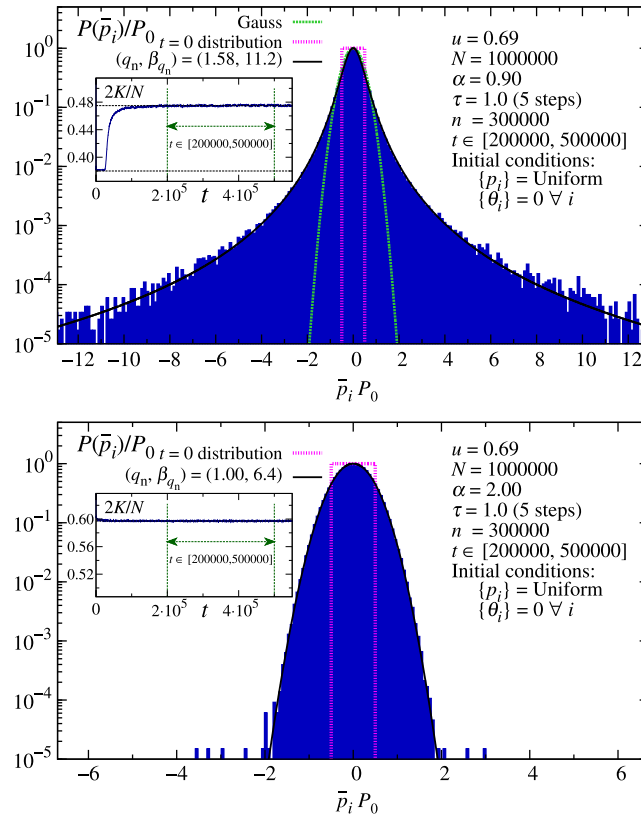


Fig. 2. A typical single-initial-condition one-momentum distribution $P(p)$ for $N = 10^6$, $u = 0.69$, $\tau = 1$ (corresponding to 5 molecular-dynamical algorithmic steps), calculated in the region $[t_{\min}, t_{\max}] = [200\,000, 500\,000]$ for $\alpha = 0.9$ (top plot), and $\alpha = 2.0$ (bottom plot). The upper temperature indicated in the $\alpha = 0.9$ inset coincides with that analytically calculated within BG statistical mechanics, namely $T_{\text{kin}} \equiv \langle 2K(t)/N \rangle \simeq 0.475$. The horizontal line of the $\alpha = 2.0$ inset corresponds to the time average calculated numerically; indeed, analytical solutions are only available for $\alpha < 1$ [23] and in the $\alpha \rightarrow \infty$ limit [24]. The continuous curves correspond to $P(\bar{p})/P_0 = e^{-\beta_{q_n}^{(p_0)} |\bar{p} P_0|^2/2}$ with $(q_n, \beta_{q_n}^{(p_0)}) = (1.58, 11.2)$ for $\alpha = 0.9$ and $(1.0, 6.4)$ for $\alpha = 2.0$. The value of q_n for $\alpha = 0.9$ corresponds to the red open circle in Fig. 3; notice that $1/\beta_{q_n}^{(p_0)} \neq T$ in this case. Each distribution has been rescaled with its own P_0 .

do exhibit $q_n \geq 7/5$. If we use a q -Gaussian $P(p)$ within Eq. (7), we obtain, through a relatively easy calculation

$$\kappa_q(q) = \frac{3 - q}{1 + q}, \tag{8}$$

as also shown in Fig. 3.

4.3. q versus α

In Figs. 4 and 5 we illustrate (q_n, β_{q_n}) as functions of (α, u, τ) for large values of N . All the $(u, \tau) = (0.69, 1)$ results for q_n have been also reported in Fig. 3. One of the interesting features that we can observe is that in all cases q_n approaches the BG value $q = 1$ when τ increases. However, this approach is nearly exponential for $(\alpha < 1, u < 0.75)$, $(\alpha > 1, u > 0.75)$, and $(\alpha > 1, u < 0.75)$, whereas it is extremely slow for $(\alpha < 1, u > 0.75)$ (notice that, in the latter case, q_n exhibits a zero slope with regard to τ at $\tau = 1$), precisely the region where the largest Lyapunov exponent approaches zero with increasing N (we remind that the $d = 1$ critical point for $0 \leq \alpha < 1$ is known to be $u_c = 3/4$). This suggests the following nonuniform convergence: $\lim_{N \rightarrow \infty} \lim_{\tau \rightarrow \infty} q_n(\alpha, u, N, \tau) = 1$ ($\forall \alpha$), whereas $\lim_{\tau \rightarrow \infty} \lim_{N \rightarrow \infty} q_n(\alpha, u, N, \tau) > 1$ (for $0 \leq \alpha < 1$). Lack of computational strength has not allowed us to directly verify this conjecture. This leaves as an interesting open question whether $\lim_{\tau \rightarrow \infty} \lim_{N \rightarrow \infty} q_n(\alpha, u, N, \tau)$ recovers $\lim_{N \rightarrow \infty} q_n(\alpha, u, N)$, where the latter would correspond to successive approximations for increasingly large N .

For all α , our numerical values of q are always larger or equal to unit. This is not mandatory for Hamiltonian systems, and neither for maps at the edge of chaos. For example, for the Fermi–Pasta–Ulam finite-size chains, values of q both above and below unity were longstandingly observed in different regions of phase space [39] (see also Ref. [40], where it is argued – disputably though – that q -exponentials with values of q above unity are not admissible within nonextensive statistics for classical many-body Hamiltonians). For the case of maps at their edge of chaos, studies exhibiting values of q both above

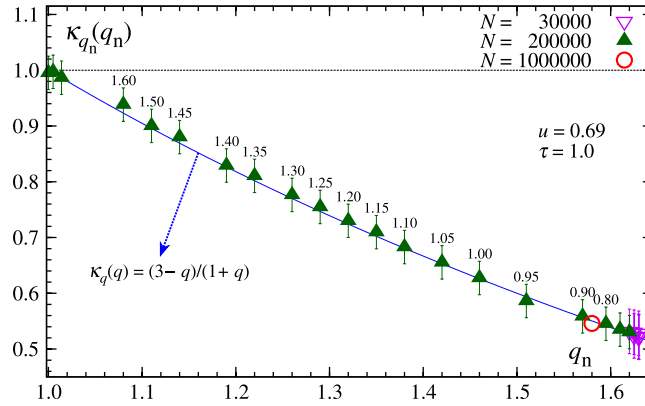


Fig. 3. q_n and q -kurtosis κ_{q_n} that have been obtained from the histograms corresponding to typical values of α (numbers indicated on top of the points). The red circle corresponds to $\alpha = 0.9$ in Fig. 2. The continuous curve $\kappa_q = (3 - q)/(1 + q)$ is the analytical one obtained with q -Gaussians. Notice that κ_q is finite up to $q = 3$ (maximal admissible value for a q -Gaussian to be normalizable), and that it does not depend on β_{q_n} . The visible departure from the dotted line at $\kappa_q = 1$ corresponding to a Maxwellian distribution, neatly reflects the departure from BG thermostatics.

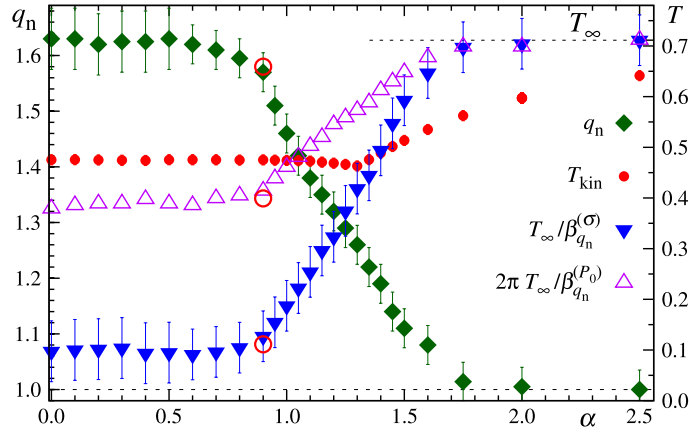


Fig. 4. α -dependences of (q_n, β_{q_n}) for $(u, \tau, N) = (0.69, 1.0, N)$, where $N = 200\,000$ ($N = 30\,000$ for $\alpha \geq 0.6$ ($\alpha \leq 0.5$), with n never smaller than 300 000. We have verified the existence of finite-size effects, in particular, for α above and close to unity, q_n slowly decreases with increasing N . Notice that $T_{\text{kin}} \simeq 0.475$ up to $\alpha \simeq 1.35$, where it starts increasing (red full circles), and, for $\alpha \gg 1$, approaches the analytical value $T_\infty = 0.7114 \dots$ [24] (by using the values that we have obtained up to $\alpha = 40$, we observe that approximately $T_\infty - T_\alpha \simeq 0.4/\alpha^2$ for $\alpha \gg 1$). The red open circles correspond to the example in Fig. 2 (also indicated in Fig. 3). The full (open) triangles have been obtained from rescaled histograms where the momenta have been divided by the standard deviation σ (multiplied by P_0 , as illustrated in Fig. 2); in other words, they both indicate (through two different normalization procedures) a single physical quantity, namely the width of the distribution. The error bars corresponding to the triangles are of the same order; the error bars of T_{kin} are of the order of the full circles (red). Naturally, $P_0 \times \sigma$ is nearly constant; to take into account the numerical deviations (from a strict constant) due to parameters such as (N, n, τ) , we have normalized both $\beta_{q_n}^{(\sigma)}$ and $\beta_{q_n}^{(P_0)}$ in such a way that the analytical value $T_\infty = 0.7114 \dots$ is recovered.

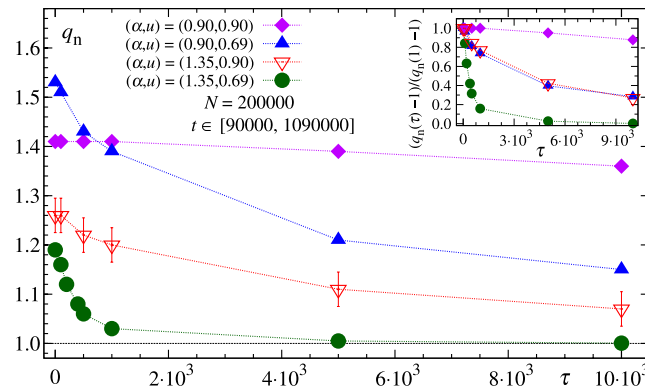


Fig. 5. τ -dependence of q_n for $N = 200\,000$, $[t_{\text{min}}, t_{\text{max}}] = [90\,000, 1090\,000]$ (hence $n = 1000\,000$ for $\tau = 1$), and typical values of u above and below the critical value $u_c = 0.75$, and of α above and below the special value $\alpha = 1$ (see Ref. [3]). All the error bars are of the same order of those indicated on the red empty triangles. *Inset:* τ -dependence of $[q_n(\tau) - 1]/[q_n(1) - 1]$.

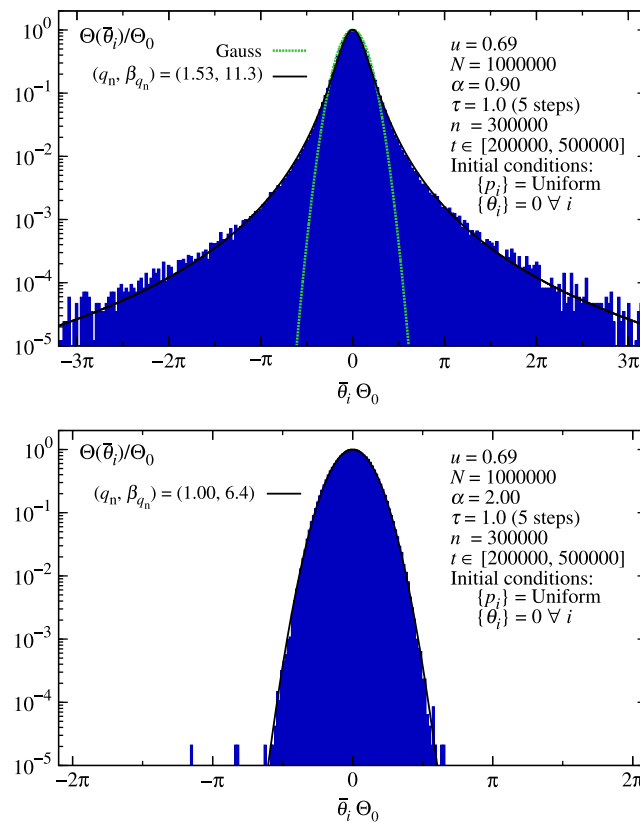


Fig. 6. A typical single-initial-condition one-angle distribution $\Theta(\theta)$ for exactly the same conditions of Fig. 2 ($\alpha = 0.9$ for the top plot; $\alpha = 2.0$ for the bottom plot). Notice that the fitting parameters (q_n, β_{q_n}) of the present q -Gaussian $\Theta(\theta) = \Theta_0 e_{q_n}^{-\beta_{q_n} |\bar{\theta}(\theta_0)|^2/2}$ (continuous curve) practically coincide with those of Fig. 2.

and below unity are also available [41,42]. Finally, q -exponential distributions of energy can also be seen in Ref. [43] for q both above and below unity.

4.4. Angle distribution

To further clarify this new thermostistical scenario it is helpful to analyze the behavior of the angles θ_i 's. In Fig. 6 we present the angle distributions obtained in exactly the same conditions of the previously shown momenta distributions (see Fig. 2). The numerical solution of the equations of motion of system (4) provides an unbound domain for the canonical variables θ_i 's, namely $\theta_i(t) \in (-\infty, +\infty)$. Notice though that the dynamics itself depends solely on the values of the phase modulo 2π since angles θ_i 's appear as arguments of sine and cosine functions. An unbound representation for the angles is quite convenient since it directly reflects the continuous rotations of the rotors (see also Ref. [44]).

4.5. Time versus ensemble averages

Let us focus on here a very interesting issue, namely the discrepancy between ensemble averages and time averages, which reveals the nonergodicity of the present system whenever the interactions are sufficiently long-ranged. This phenomenon occurs, interestingly enough, *even after the kinetic temperature has reached its BG value*. In Fig. 7, time and ensemble averages are compared for $\alpha = 0.9$ and $N = 200\,000$. The initial conditions are the same used in the previous results, namely the system starts with magnetization $M = 1$, which is followed by a violent relaxation, bringing it to the QSS. Though N is considerably large, the QSS duration is relatively short since $\alpha = 0.9$. After this short QSS period, the system exhibits a crossover to the BG kinetic temperature. As indicated in the top of Fig. 7, photographs of the velocities of all the particles were taken at $t = 90\,000$, $240\,000$ and $360\,000$. In order to approach an *ensemble average*, this procedure was repeated for 50 realizations and the histograms of the velocities were calculated through simple (arithmetic) means (see Fig. 7(a, b, c)). For one of these realizations, a *time average* was calculated within the interval $t \in [90\,000, 360\,000]$ (see Fig. 7(d)).

The interesting and deep discrepancy that we observe here between time and ensemble averages (i.e., lack of ergodicity) for relatively small values of α is consistent with what was previously obtained [45] for $\alpha = 0$ and small values of N

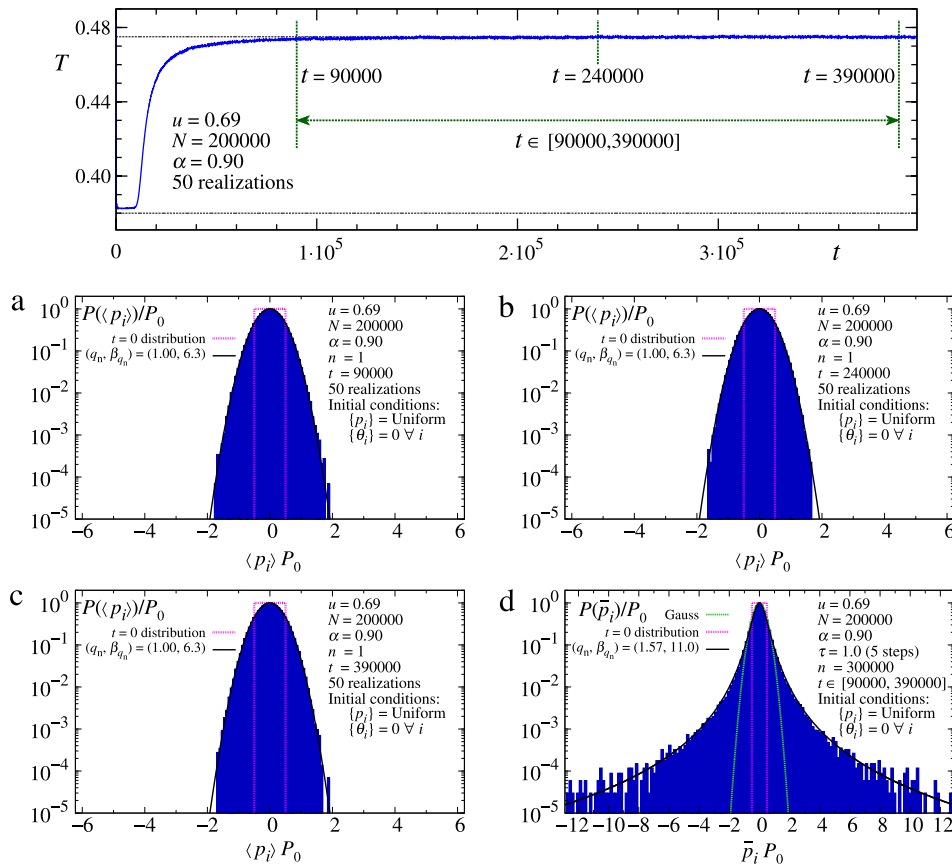


Fig. 7. Top figure: Time evolution of the kinetic temperature T for $(\alpha, u, N) = (0.90, 0.69, 200\,000)$ averaged over 50 different realizations, i.e., we run the system 50 times with different seeds of the random number generator for the initial uniform velocity distribution. After that, a simple (arithmetic) average has been calculated. One of these 50 realizations was also shown in Fig. 1. Panels (a), (b) and (c): The averages over these 50 realizations of the momenta distribution (by $\langle p \rangle$ we denote the average over the realizations) at three distinct times, namely at $t = 90\,000$, $t = 240\,000$ and $t = 390\,000$, as indicated in the top figure. Let us mention that the Gaussian shape of these averaged distributions remains essentially the same from a few realizations on; in other words, 50 realizations is largely above what would be numerically necessary in order to have invariant results. Panel (d): Time average calculated within the interval $t \in [900\,000, 390\,000]$ for a single realization. Let us stress that the q -Gaussian shape becomes increasingly better (especially in the tails) with increasing N , as can be seen by comparing the present figure (d) with Fig. 2 (top). Although not shown here, all the corresponding panels (a–d) essentially coincide among them for α large enough (say $\alpha = 2$), and they provide a Gaussian shape, as expected for an ergodic system.

($N = 100$ in that case; see Fig. 4 in Ref. [45]). Actually, the study reported in Ref. [45] mainly focused on the QSS regime of the HMF system (see also Ref. [46] as well as Ref. [47]). It was later clarified [48] that, for $(\alpha, u) = (0, 0.69)$ and N up to $N \approx 20\,000$, one can distinguish three classes of QSS events (which were referred to as classes 1, 2 and 3) whenever the system starts with a water-bag initial condition as described in the above Section 4. In Ref. [48], the q -Gaussian one-momentum distributions were obtained for the class 1 events. It was, however, verified that, for increasingly large N , many of the QSS events belong to class 3. Let us mention by the way that the only type of events investigated here precisely are those of class 3: typical $\alpha < 1$ patterns are included in Fig. 1.

5. Final remarks

Summarizing, it has been observed for at least one decade that, for $0 \leq \alpha < 1$, the longstanding QSSs of the present model (i.e., the α -XY system of rotators) exhibit anomalous distributions (Vlasov-like for some classes of initial conditions, and different, including q -Gaussian-shaped, ones for other classes) for the momenta of the rotators, whereas nothing particularly astonishing was expected to occur once the system had done the crossover to the (presumably stationary) state whose kinetic temperature coincides with that analytically obtained within the BG theory.

The present results (obtained from first principles, i.e., using essentially nothing but Newton’s law) neatly show that, if time is large enough so that the kinetic-temperature crossover has occurred (as illustrated in the Inset of Fig. 2), the situation is far more complex. Indeed, robust and longstanding q -Gaussian distributions are numerically observed under a wide variety of situations. The fact that the numerical kinetic temperature be the one predicted within the BG theory is sometimes thought as a sufficient condition for standard statistical mechanics to be applicable. However, the lack of ergodicity caused by the long-range nature of the interactions shows that, at the time range we are focusing on [49], the discussion is more subtle.

Indeed, the shape of the momenta distributions can considerably and longstandingly differ from Gaussians, and it is only when the correlations become negligible (i.e., when $\tau \gg 1$ and/or $\alpha \gg 1$) that the classical Maxwellian distribution (with $\beta_{qm}^{-1} = T$) is (numerically) recovered. Similar results are also observed for the angle distributions, as illustrated in Fig. 6. The full discussion of the angle distributions is out of the scope of the present paper and will be discussed in detail elsewhere.

Let us mention at this point that the breakdown of ergodicity which emerges for $\alpha/d \leq 1$ [45,48,50] as indicated in Fig. 7 is neatly worthy of further consideration (see also, for a quantum system, [51]). Indeed, within the BG framework, not only the kinetic temperature (or the magnetization) must coincide with the canonical prediction, but a Maxwellian form also is expected in the velocity distribution, independently on whether it is time or ensemble averages which are being calculated. However, we have shown that long-range interactions make the physical scenario much more delicate. It is the aim of nonextensive statistical mechanics [2,6] to provide a possible frame for discussing such difficult cases. Within this generalized theory, a plausible thermostatical scenario could be as follows. The stationary state is expected to yield a probability distribution $e_q^{-\beta_q \mathcal{H}} / Z_q(\beta_q)$ with $Z_q(\beta_q) \equiv \int dp_1 \dots dp_N d\theta_1 \dots d\theta_N e_q^{-\beta_q \mathcal{H}}$. The index q is expected to characterize universality classes, possibly a function $q(\alpha/d)$ to be different from 1 for $0 \leq \alpha/d < 1$, and equal to 1 for $\alpha/d \geq 1$. If this is so, an interesting quantity would of course be the one-momentum marginal probability $P(p_1) = \int dp_2 \dots dp_N d\theta_1 \dots d\theta_N e_q^{-\beta_q \mathcal{H}} / Z_q$. The functional form of $P(p_1)$ is unknown. A possibility could however be that, in the $N \rightarrow \infty$ limit, we simply have $P(p_1) \propto e_{q_m}^{-\beta_{q_m} p_1^2/2}$, i.e., a q_m -Gaussian form, where m stands for *momentum*. Indeed, q -Gaussians emerge extremely frequently in complex systems (see, e.g., [8–11,39,41,42,52–56]; see also [57–63] for high energy physics). The index q_m could depend not only on α/d , but also, in principle, on u . Similar considerations are in order for the one-angle marginal probability $\Theta(\theta_1) = \int dp_1 \dots dp_N d\theta_2 \dots d\theta_N e_q^{-\beta_q \mathcal{H}} / Z_q$, whose precise analytical form also is unknown.

The present example, with its neat and sensible drift from BG behavior for short-range interactions to non-BG behavior for long-range interactions, constitutes a novel illustration of the great thermostatical richness that a breakdown of ergodicity can cause. It also serves as an invitation for deeper analysis of the thermal statistics of all those very many models in the literature that are definitively nonergodic (e.g., glasses, spin-glasses, among others), and for which, nevertheless, the BG theory is straightforwardly used without further justification. It illustrates Gibbs' remark [1] that standard statistical mechanics are not justified whenever the canonical partition function diverges (which is the case for long-range interactions, i.e., for $0 \leq \alpha \leq 1$).

Acknowledgements

We acknowledge useful conversations with M. Jauregui, L.G. Moyano, F.D. Nobre, A. Pluchino, A. Rapisarda and L.A. Rios. We have benefited from partial financial support by CNPq, Faperj and Capes (Brazilian Agencies).

References

- [1] J.W. Gibbs, *Elementary Principles in Statistical Mechanics – Developed with Especial Reference to the Rational Foundation of Thermodynamics*, C. Scribner's Sons, New York, 1902. Yale University Press, New Haven, 1948; OX Bow Press, Woodbridge, Connecticut, 1981. "In treating of the canonical distribution, we shall always suppose the multiple integral in equation (92) (the partition function) to have a finite value, as otherwise the coefficient of probability vanishes, and the law of distribution becomes illusory. This will exclude certain cases, but not such apparently, as will affect the value of our results with respect to their bearing on thermodynamics. It will exclude, for instance, cases in which the system or parts of it can be distributed in unlimited space [...]. It also excludes many cases in which the energy can decrease without limit, as when the system contains material points which attract one another inversely as the squares of their distances [...]. For the purposes of a general discussion, it is sufficient to call attention to the assumption implicitly involved in the formula (92)".
- [2] C. Tsallis, *Introduction to Nonextensive Statistical Mechanics Approaching a Complex World*, Springer, New York, 2009.
- [3] C. Anteneodo, C. Tsallis, Breakdown of exponential sensitivity to initial conditions: role of the range of interactions, *Phys. Rev. Lett.* 80 (1998) 5313.
- [4] M. Antoni, S. Ruffo, Clustering and relaxation in Hamiltonian long-range dynamics, *Phys. Rev. E* 52 (1995) 2361.
- [5] P.H. Chavanis, A. Campa, Inhomogeneous Tsallis distributions in the HMF model, *Eur. Phys. J. B* 76 (2010) 581.
- [6] C. Tsallis, Possible generalization of Boltzmann–Gibbs statistics, *J. Stat. Phys.* 52 (1988) 479.
- [7] A regularly updated bibliography on nonextensive statistical mechanics and nonadditive entropies is available at <http://tsallis.cat.cbpf.br/biblio.htm>.
- [8] J.S. Andrade, G.F.T da Silva, A.A. Moreira, F.D. Nobre, E.M.F. Curado, Thermostatistics of overdamped motion of interacting particles, *Phys. Rev. Lett.* 105 (2010) 01; Andrade, et al., *Phys. Rev. Lett.* 107 (2011) 088902. Reply; Y. Levin, R. Pakter, Comment on "thermostatistics of overdamped motion of interacting particles", *Phys. Rev. Lett.* 107 (2011) 088901.
- [9] M.S. Ribeiro, F.D. Nobre, E.M.F. Curado, Time evolution of interacting vortices under overdamped motion, *Phys. Rev. E* 85 (2012) 021146.
- [10] M.S. Ribeiro, F.D. Nobre, E.M.F. Curado, Overdamped motion of interacting particles in general confining potentials: time-dependent and stationary-state analyses, *Eur. Phys. J. B* 85 (2012) 399.
- [11] G.A. Casas, F.D. Nobre, E.M.F. Curado, Entropy production and nonlinear Fokker–Planck equations, *Phys. Rev. E* 86 (2012) 061136.
- [12] P. Jund, S.G. Kim, C. Tsallis, Crossover from extensive to nonextensive behavior driven by long-range interactions, *Phys. Rev. B* 52 (1995) 50.
- [13] F. Tamarit, C. Anteneodo, Rotators with long-range interactions: connection with the mean-field approximation, *Phys. Rev. Lett.* 84 (2000) 208.
- [14] A. Campa, A. Giansanti, D. Moroni, Canonical solution of a system of long-range interacting rotators on a lattice, *Phys. Rev. E* 62 (2000) 303.
- [15] J.R. Grigera, Extensive and non-extensive thermodynamics, a molecular dynamic test, *Phys. Lett. A* 217 (1996) 47–51.
- [16] S.A. Cannas, F.A. Tamarit, Long-range interactions and nonextensivity in ferromagnetic spin systems, *Phys. Rev. B* 54 (1996) R12661–R12664.
- [17] L.C. Sampaio, M.P. de Albuquerque, F.S. de Menezes, Nonextensivity and Tsallis statistics in magnetic systems, *Phys. Rev. B* 55 (1997) 5611.
- [18] R.F.S. Andrade, S.T.R. Pinho, Tsallis scaling and the long-range Ising chain: a transfer matrix approach, *Phys. Rev. E* 71 (2005) 026126.
- [19] C.A. Condat, J. Rangel, P.W. Lamberti, Anomalous diffusion in the nonasymptotic regime, *Phys. Rev. E* 65 (2002) 026138.
- [20] U.L. Fulco, L.R. Silva, F.D. Nobre, H.H.A. Rego, L.S. Lucena, Effects of site dilution on the one-dimensional long-range bond-percolation problem, *Phys. Lett. A* 312 (2003) 331–335.

- [21] H.H.A. Rego, L.S. Lucena, L.R. Silva, C. Tsallis, Crossover from extensive to nonextensive behavior driven by long-range $d = 1$ bond percolation, *Physica A* 266 (1999) 42.
- [22] A. Campa, A. Giansanti, D. Moroni, Canonical solution of classical magnetic models with long-range couplings, *J. Phys. A* 36 (2003) 6897.
- [23] A. Giansanti, D. Moroni, A. Campa, Universal behaviour in the static and dynamic properties of the α -XY model, *Chaos Solitons Fractals* 13 (2002) 407.
- [24] D.C. Mattis, Transfer matrix in plane-rotator model, *Phys. Lett. A* 104 (1984) 357; *The Theory of Magnetism Made Simple: An Introduction to Physical Concepts and to Some Useful Mathematical Methods*, World Scientific, Singapore, 2006.
- [25] A. Campa, A. Giansanti, D. Moroni, C. Tsallis, Classical spin systems with long-range interactions: universal reduction of mixing, *Phys. Lett. A* 286 (2001) 251.
- [26] B.J.C. Cabral, C. Tsallis, Metastability and weak mixing in classical long-range many-rotator systems, *Phys. Rev. E* 66 (2002) 065101.
- [27] H. Yoshida, Construction of higher order symplectic integrators, *Phys. Lett. A* 150 (1990) 262.
- [28] To implement the fast Fourier transform for the α -XY model we have used the FFTW library.
- [29] S. Umarov, C. Tsallis, S. Steinberg, On a q -central limit theorem consistent with nonextensive statistical mechanics, *Milan J. Math.* 76 (2008) 307; S. Umarov, C. Tsallis, M. Gell-Mann, S. Steinberg, Generalization of symmetric alpha-stable Lévy distributions for $q > 1$, *J. Math. Phys.* 51 (2010) 33502. It was (correctly) pointed by H.J. Hilhorst in [30] that, in their present form, these proofs contain a gap, as they use the inverse q -Fourier transform, which generically is not unique. It was subsequently shown in [31] and in [32] that supplementary information determines a *unique* inverse q -Fourier transform. The inclusion of this fact within those proofs remains to be done. Nevertheless, in [33] and in [34] there exist different proofs of essentially the same thesis *without* using q -Fourier transforms.
- [30] H.J. Hilhorst, Note on a q -modified central limit theorem, *J. Stat. Mech.* 10 (2010) P10023.
- [31] M. Jauregui, C. Tsallis, E.M.F. Curado, q -moments remove the degeneracy associated with the inversion of the q -Fourier transform, *J. Stat. Mech.* 10 (2011) P10016; M. Jauregui, C. Tsallis, q -generalization of the inverse Fourier transform, *Phys. Lett. A* 375 (2011) 2085.
- [32] A. Plastino, M.C. Rocca, q -Fourier transform and its inversion-problem, *Milan J. Math.* 80 (2012) 243–249; Inversion of Umarov–Tsallis–Steinberg’s q -Fourier transform and the complex-plane generalization, *Physica A* 391 (2012) 4740.
- [33] C. Vignat, A. Plastino, Central limit theorem and deformed exponentials, *J. Phys. A* 40 (2007) F969; Geometry of the central limit theorem in the nonextensive case, *Phys. Lett. A* 373 (2009) 1713.
- [34] M.G. Hahn, X. Jiang, S. Umarov, On q -Gaussians and exchangeability, *J. Phys. A* 43 (2010) 165208.
- [35] For $q = 2$, the q -Gaussian corresponds to the well known Cauchy–Lorentz distribution (Cauchy distribution as called by mathematicians, and Lorentzian as called by physicists). The q -Gaussian distributions include as particular cases the r - and the Student’s t -distributions [64], and, in the $q \rightarrow 1$ limit, recover the Gaussian. q -Gaussians and the related q -exponentials appear in a variety of phenomena, from biology [65] and economics [66] to astronomy [67] and high energy physics [58–63].
- [36] C. Tsallis, A. Plastino, R. Alvarez-Estrada, Escort mean values and the characterization of power-law-decaying probability densities, *J. Math. Phys.* 50 (2009) 043303; B. Coutinho dos Santos, C. Tsallis, Time evolution towards q -Gaussian stationary states through unified Itô–Stratonovich stochastic equation, *Phys. Rev. E* 82 (2010) 061119.
- [37] C. Beck, F. Schögl, *Thermodynamics of Chaotic Systems: An Introduction*, Cambridge University Press, Cambridge, 1995.
- [38] C. Tsallis, R.S. Mendes, A.R. Plastino, The role of constraints within generalized nonextensive statistics, *Physica A* 261 (1998) 534.
- [39] M. Leo, R.A. Leo, P. Tempesta, Thermostatistics in the neighbourhood of the π -mode solution for the Fermi–Pasta–Ulam β system: from weak to strong chaos, *J. Stat. Mech.* 04 (2010) P04021; M. Leo, R.A. Leo, P. Tempesta, C. Tsallis, Non-Maxwellian behavior and quasistationary regimes near the modal solutions of the Fermi–Pasta–Ulam β system, *Phys. Rev. E* 85 (2012) 031149.
- [40] J.F. Lutsko, J.P. Boon, P. Grosfils, Is the Tsallis entropy stable? *Europhys. Lett.* 86 (2009) 40005; J.F. Lutsko, J.P. Boon, Questioning the validity of non-extensive thermodynamics for classical Hamiltonian systems, *Europhys. Lett.* 95 (2011) 20006; J.F. Lutsko, J.P. Boon, Nonextensive formalism and continuous Hamiltonian systems, *Phys. Lett. A* 375 (2011) 329.
- [41] U. Tirnakli, C. Tsallis, C. Beck, Closer look at time averages of the logistic map at the edge of chaos, *Phys. Rev. E* 79 (2009) 056209; O. Afsar, U. Tirnakli, Probability densities for the sums of iterates of the sine-circle map in the vicinity of the quasiperiodic edge of chaos, *Phys. Rev. E* 82 (2010) 046210.
- [42] A. Pluchino, A. Rapisarda, C. Tsallis, Noise, synchrony, and correlations at the edge of chaos, *Phys. Rev. E* 87 (2013) 022910.
- [43] M. Campisi, F. Zhan, P. Hänggi, On the origin of power laws in equilibrium, *Europhys. Lett.* 99 (2012) 60004.
- [44] L.G. Moyano, C. Anteneodo, Diffusive anomalies in a long-range Hamiltonian system, *Phys. Rev. E* 74 (2006) 021118.
- [45] A. Pluchino, A. Rapisarda, C. Tsallis, Nonergodicity and central-limit behavior for long-range Hamiltonians, *Europhys. Lett.* 80 (2007) 26002.
- [46] A. Campa, P.H. Chavanis, Caloric curves fitted by polytropic distributions in the HMF model, *Eur. Phys. J. B* 86 (2013) 1–29.
- [47] P.H. Chavanis, Kinetic theory of spatially inhomogeneous stellar systems without collective effects, 2012. arXiv:1210.5743 [astro-ph.GA].
- [48] A. Pluchino, A. Rapisarda, C. Tsallis, A closer look at the indications of q -generalized central limit theorem behavior in quasi-stationary states of the HMF model, *Physica A* 387 (2008) 3121; Comment on “ergodicity and central-limit theorem in systems with long-range interactions” by A. Figueiredo, et al., *Europhys. Lett.* 85 (2009) 60006.
- [49] It is of course conceivable that, for $0 \leq \alpha/d \leq 1$ in the ordered limit $\lim_{N \rightarrow \infty} \lim_{t \rightarrow \infty}$ as well as for $\alpha/d > 1$ in any of the $(N, t) \rightarrow (\infty, \infty)$ limits, the Maxwellian distributions typical of thermal equilibrium are eventually recovered. However, the present work shows that, even for very large values of (N, t) , this ultimate situation might be amazingly slow to be achieved (analogously to what occurs in systems such as those discussed in Ref. [68]). In fact, the thermostats of complex systems such as the present one can be very rich, exhibiting more than one temperature, namely the kinetic as well as a different, effective one [8–11,69]. Such feature could be an indication of some sort of dissipative phenomenon at some mesoscopic level.
- [50] A. Figueiredo, T.M.R. Filho, M.A. Amato, Ergodicity and central-limit theorem in systems with long-range interactions, *Europhys. Lett.* 83 (2008) 30011; Reply to the comment A. Pluchino, et al., *Europhys. Lett.* 85 (2009) 60007.
- [51] C. Brukner, A. Zeilinger, Conceptual inadequacy of the Shannon information in quantum measurements, *Phys. Rev. A* 63 (2001) 022113.
- [52] E. Lutz, Anomalous diffusion and Tsallis statistics in an optical lattice, *Phys. Rev. A* 67 (2003) 051402; P. Douglas, S. Bergamini, F. Renzoni, Tunable Tsallis distributions in dissipative optical lattices, *Phys. Rev. Lett.* 96 (2006) 110601.
- [53] B. Liu, J. Goree, Superdiffusion and non-Gaussian statistics in a driven-dissipative $2d$ dusty plasma, *Phys. Rev. Lett.* 100 (2008) 055003.
- [54] R.G. DeVoe, Power-law distributions for a trapped ion interacting with a classical buffer gas, *Phys. Rev. Lett.* 102 (2009) 063001.
- [55] G. Miritello, A. Pluchino, A. Rapisarda, Central limit behavior in the Kuramoto model at the “edge of chaos”, *Physica A* 388 (2009) 4818.
- [56] E. Lutz, Anomalous diffusion and Tsallis statistics in an optical lattice, *Phys. Rev. A* 67 (2003) 051402; P. Douglas, S. Bergamini, F. Renzoni, Tunable Tsallis distributions in dissipative optical lattices, *Phys. Rev. Lett.* 96 (2006) 110601.
- [57] C. Tsallis, J.C. Anjos, E.P. Borges, Fluxes of cosmic rays: a delicately balanced stationary state, *Phys. Lett. A* 310 (2003) 372.
- [58] C.-Y. Wong, G. Wilk, Tsallis fits to p_T spectra for pp collisions at LHC, *Acta Phys. Polon. B* 43 (2012) 2043; Tsallis fits to p_T spectra and multiple hard scattering in pp collisions at the LHC, *Phys. Rev. D* 87 (2013) 114007.
- [59] V. Khachatryan, et al., (CMS Collaboration), Transverse-momentum and pseudorapidity distributions of charged hadrons in pp collisions at $\sqrt{s} = 7$ TeV, *Phys. Rev. Lett.* 105 (2010) 1; Transverse-momentum and pseudorapidity distributions of charged hadrons in pp collisions at $\sqrt{s} = 0.9$ and 2.36 TeV, *J. High Energy Phys.* 02 (2010) 041; Observation of long-range, near-side angular correlations in proton–proton collisions at the LHC, *J. High Energy Phys.* 09 (2010) 091; Strange particle production in pp collisions at $\sqrt{s} = 0.9$ and 7 TeV, *J. High Energy Phys.* 05 (2011) 064; Charged particle transverse momentum spectra in pp collisions at $\sqrt{s} = 0.9$ and 7 TeV, *J. High Energy Phys.* 08 (2011) 086.

- [60] K. Aamodt, et al., (ALICE Collaboration), Transverse momentum spectra of charged particles in proton–proton collisions at $\sqrt{s} = 900$ GeV with ALICE at the LHC, Phys. Lett. B 693 (2010) 53; Production of pions, kaons and protons in pp collisions at $\sqrt{s} = 900$ GeV with ALICE at the LHC, Eur. Phys. J. C 71 (2011) 1655; Strange particle production in proton–proton collisions at $\sqrt{s} = 09$ with ALICE at the LHC, Eur. Phys. J. C 71 (2011) 1.
- [61] B. Abelev, et al., (ALICE Collaboration), Measurement of electrons from semileptonic heavy-flavor hadron decays in pp collisions at $\sqrt{s} = 7$ TeV, Phys. Rev. D 86 (2012) 112007.
- [62] G. Aad, et al., (ATLAS Collaboration), Charged-particle multiplicities in pp interactions measured with the ATLAS detector at the LHC, New J. Phys. 13 (2011) 053033.
- [63] A. Adare, et al., (PHENIX Collaboration), Measurement of neutral mesons in $p + p$ collisions at $\sqrt{s} = 200$ GeV and scaling properties of hadron production, Phys. Rev. D 83 (2011) 052004; Nuclear modification factors of ϕ mesons in $d + Au$, $Cu + Cu$, and $Au + Au$ collisions at $\sqrt{s_{NN}} = 200$ GeV, Phys. Rev. C 83 (2011) 024909; Identified charged hadron production in $p + p$ collisions at $\sqrt{s} = 200$ and 62.4 GeV, Phys. Rev. C 83 (2011) 064903; Production of ω mesons in $p + p$, $d + Au$, $Cu + Cu$, and $Au + Au$ collisions at $\sqrt{s_{NN}} = 200$ GeV, Phys. Rev. C 84 (2011) 044902.
- [64] A.M.C. Souza, C. Tsallis, Student's t - and r -distributions: unified derivation from an entropic variational principle, Physica A 236 (1997) 52.
- [65] A. Upadhyaya, J.-P. Rieu, J.A. Glazier, Y. Sawada, A. Upadhyaya, J.-P. Rieu, J.A. Glazier, Y. Sawada, Anomalous diffusion and non-Gaussian velocity distribution of Hydra cells in cellular aggregates, Physica A 293 (2001) 549.
- [66] J. Kwapien, S. Drożdż, Physical approach to complex systems, Phys. Rep. 515 (2012) 115.
- [67] A.S. Betzler, E.P. Borges, Nonextensive distributions of asteroid rotation periods and diameters, Astron. Astrophys. 539 (2012) A158.
- [68] V. Schwämmle, F.D. Nobre, C. Tsallis, q -Gaussians in the porous-medium equation: stability and time evolution, Eur. Phys. J. B 66 (2008) 537.
- [69] W. Niedenzu, T. Griebner, H. Ritsch, Kinetic theory of cavity cooling and self-organisation of a cold gas, Europhys. Lett. 96 (2011) 43001; L. Rios, R. Galvão, L. Cirto, Comment on “Debye shielding in a nonextensive plasma”, Phys. Plasmas 19 (2012) 034701. Phys. Plasmas 18 (2011) 062102.